

Highly Efficient Large Bite Angle Diphosphine Substituted Molybdenum Catalyst for Hydrosilylation

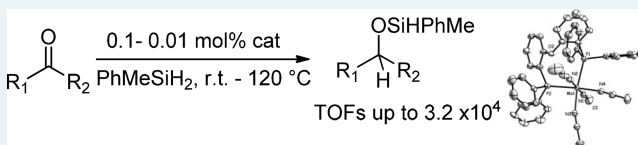
Subrata Chakraborty, Olivier Blacque, Thomas Fox, and Heinz Berke*

Institute of Inorganic Chemistry, University of Zürich, Winterthurerstrasse 190, CH-8057 Zürich, Switzerland

S Supporting Information

ABSTRACT: Treatment of the complex $\text{Mo}(\text{NO})(\text{NCMe})_2\text{Cl}_2$ with the large bite angle diphosphine, 2,2'-bis(diphenylphosphino)diphenylether (DPEphos) afforded the dinuclear species $[\text{Mo}(\text{NO})(\text{P}(\text{OP})\text{Cl}_2)_2][\mu\text{Cl}]_2$ ($\text{P}(\text{OP}) = \text{DPEphos} = (\text{Ph}_2\text{PC}_6\text{H}_4)_2\text{O}$ (**1**)). **1** could be reduced in the presence of Zn and MeCN to the cationic complex $[\text{Mo}(\text{NO})(\text{P}(\text{OP})(\text{NCMe})_3)^+[\text{Zn}_2\text{Cl}_6]^{2-}_{1/2}]$ (**2**). In a metathetical reaction the $[\text{Zn}_2\text{Cl}_6]^{2-}_{1/2}$ counteranion was replaced with $\text{NaBAR}^{\text{F}}_4$ ($\text{BAR}^{\text{F}}_4 = [\text{B}\{3,5-(\text{CF}_3)_2\text{C}_6\text{H}_3\}_4]^-$) to obtain the $[\text{BAR}^{\text{F}}_4]^-$ salt $[\text{Mo}(\text{NO})(\text{P}(\text{OP})(\text{NCMe})_3)^+[\text{BAR}^{\text{F}}_4]^-]$ (**3**). **3** was found to catalyze hydrosilylations of various *para* substituted benzaldehydes, cyclohexanecarboxaldehyde, 2-thiophenecarboxaldehyde, and 2-furfural at 120 °C. A screening of silanes revealed primary and secondary aromatic silanes to be most effective in the catalytic hydrosilylation with **3**. Also ketones could be hydrosilylated at room temperature using **3** and PhMeSiH_2 . A maximum turnover frequency (TOF) of $3.2 \times 10^4 \text{ h}^{-1}$ at 120 °C and a TOF of 4400 h^{-1} was obtained at room temperature for the hydrosilylation of 4-methoxyacetophenone using PhMeSiH_2 in the presence of **3**. Kinetic studies revealed the reaction rate to be first order with respect to the catalyst and silane concentrations and zero order with respect to the substrate concentrations. A Hammett study for various *para* substituted acetophenones showed linear correlations with negative ρ values of -1.14 at 120 °C and -3.18 at room temperature.

KEYWORDS: homogeneous catalysis, hydrosilylation, molybdenum, diphosphine, aldehydes, ketones



INTRODUCTION

The hydrosilylation of unsaturated carbonyl functionalities has received considerable attention as a convenient reduction method both in industry and in academia. In addition the alkoxy silane products obtained by atom-economical hydrosilylation are valuable intermediates for the synthesis of organosilicon polymers. Metal mediated hydrosilylation reactions generally operate according to the Chalk–Harrod mechanism for alkenes and alkynes¹ or for carbonyl compounds^{2,3} on the Ojima mechanism showing the following key steps: (a) oxidative addition of a Si–H bond to a metal center, (b) coordination of the unsaturated substrate, (c) migration of the hydride (or in rare cases of the silyl group) to the unsaturated substrate, and finally (d) reductive elimination of a C–O–Si (or C–C–Si) bond to form the hydrosilylated product. Early transition metal systems deviate from this scheme and catalyze hydrosilylation reactions via σ bond metathesis.⁴ Toste^{5a} et al demonstrated that hydrosilylation of organic carbonyls could take place via initial insertion into the Re–H bond of the $\text{Re}(\text{O})(\text{OSiPhMe}_2)(\text{PPh}_3)_2(\text{I})(\text{H})$ complex obtained via the reaction of $\text{Re}(\text{O})_2(\text{PPh}_3)_2\text{I}$ and PhMe_2SiH . In 2011, Nikonov^{5d} et al. provided evidence that the hydride transfer to carbonyl from $\text{Re}(\text{O})(\text{OSiPhMe}_2)(\text{PPh}_3)_2(\text{I})(\text{H})$ complex is not the dominant reaction pathway of the catalytic cycle. A pathway with a silylene intermediate was also proposed by Tilley et al.⁶ Asymmetric hydrosilylation with high enantioselectivities,⁷ ionic hydrosilylations⁸ with heterolysis of

the Si–H bond, and Lewis acid⁹ catalyzed hydrosilylation reactions are also well documented by several authors.

Nevertheless, to date the most common and efficient catalysts involved in hydrosilylation reactions are based on platinum group transition metals, which suffer from high cost and recognized toxicities,¹⁰ since in many cases the catalytic metal content cannot be removed from the product. To overcome this problem, the development of iron catalysts¹¹ and early transition metal catalysts¹² have attracted significant attention. Pursuing the issue of “Cheap Metals for Noble Tasks”,¹³ catalysis based on molybdenum is also quite appealing. There are several reports on Mo catalyzed hydrosilylation reactions of carbonyl compounds including in depth mechanistic investigations.^{14,15} Despite the ability of these catalysts to perform hydrosilylation reactions under mild conditions, they lack high activity and catalyst stability.

Our group has a long-standing interest in rhenium and group VI nitrosyl chemistry. Recently we had discovered excellent catalytic performance of ligand tuned rhenium nitrosyl complexes in hydrogenations¹⁶ comparable or even superior to precious metal catalysts. Hydrosilylations,¹⁷ dehydrogenative silylations,¹⁸ and dehydrogenative aminoborane coupling¹⁹ reactions and also of molybdenum catalyzed hydrogenation reactions²⁰ could be accomplished. We were particularly

Received: June 4, 2013

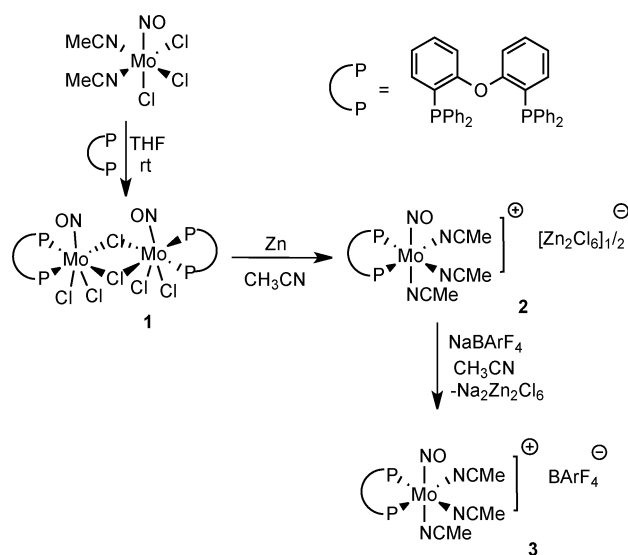
Revised: August 7, 2013

interested in developing an efficient molybdenum nitrosyl based catalyst for hydrosilylation reactions. We sought inspiration particularly from the earlier work of our group with rhenium compounds²¹ where large bite angle chelating diphosphine ligands had dramatically influenced the ability of ligand exchanges of the metal centers and directed these toward catalysis of the hydrogenation of alkenes. For this reason, we have initially chosen the simplest of aryl substituted diphosphines, the large bite angle 2,2'-bis(diphenylphosphino)-diphenylether ligand (DPEphos), and prepared molybdenum nitrosyl derivatives and applied them in efficient hydrosilylation reactions of various substituted aromatic aldehydes and ketones.

RESULTS AND DISCUSSION

Preparation of Molybdenum Nitrosyl Complexes. The preparation of the large bite angle DPEphos ligand (DPEphos = (Ph₂PC₆H₄)₂O, Bite angle = 102.2°)^{22a} containing dinuclear species [Mo(NO)(PNP)Cl₂]₂[μCl]₂ (**1**) was achieved by ligand substitution reactions starting from the Mo(NO)Cl₃(NCMe)₂ precursor complex at room temperature in tetrahydrofuran (THF) (Scheme 1). **1** precipitated out from THF solution as a

Scheme 1. Synthetic Access to Various Molybdenum Complexes with the DPEphos Ligand



gray material in 86% yield. It is insoluble in organic solvents. Therefore, it could be characterized only by elemental analysis and solid state IR spectroscopy. The IR spectrum showed a sharp signal at 1664 cm⁻¹ attributed to the ν_{NO} vibration. An attempt to cleave this chloride dinuclear species **1** by heating it in the coordinating solvent MeCN failed, which resulted in an inseparable mixture of decomposition products including the presence of the free DPEphos ligand as indicated by ³¹P NMR spectroscopy. It should be mentioned that an attempt to prepare a similar large bite angle complex using the diphosphine 4,6-bis(diphenylphosphino)-10,10-dimethylphenoxasilin(Sixanthphos) ligand^{22a} from the Mo(NO)Cl₃(NCMe)₂ precursor failed completely, even at higher temperatures as revealed by the ³¹P NMR spectra.

Despite its insolubility, the Mo(II) complex **1** could be reduced by Zn to obtain a low-valent molybdenum nitrosyl complex. The reduction of **1** with excess zinc (10 equiv) in

MeCN at room temperature led to formation of the red cationic [Mo(NO)(PNP)(NCMe)₃]⁺[Zn₂Cl₆]²⁻ complex **2** in excellent yield (84%) (Scheme 1). The ³¹P{¹H} NMR spectra revealed a single resonance at δ = 53.5 ppm, which spoke for the equivalence of the phosphorus atoms of the DPEphos ligand. A ν_{NO} band was observed at 1593 cm⁻¹. One broad signal at δ = 2.01 ppm in the ¹H NMR spectra was attributed to the methyl protons of the coordinated MeCN ligands. The signals of the C_{Me} and C_{CN} atom appeared in the ¹³C{¹H} NMR spectra at δ = 0.65 and 123 ppm, respectively. The complex was further characterized by C,H correlation, long-range C,H correlation experiments, elemental analysis, and finally by a single crystal X-ray diffraction study. **2** is soluble in MeCN, THF, and sparingly soluble in toluene.

Single crystals for a X-ray diffraction study could be obtained by layering pentane onto a concentrated toluene solution of **2** at -30 °C. The X-ray diffraction study of **2** revealed a pseudo octahedral geometry around the metal center (see Supporting Information). Two coordinated MeCN ligands occupy the plane of the DPEphos ligand. The average Mo–N_{MeCN} bond length is 2.172(5) Å. The asymmetric unit contains one cationic molybdenum molecule, one toluene as solvate, and half of the dianionic [Zn₂Cl₆]²⁻ species.

We chose the bulky noncoordinating [B{3,5-(CF₃)₂C₆H₃}]⁻ anion (BARF₄⁻) to replace the [Zn₂Cl₆]²⁻ species since exchange of the counteranion could help to increase the solubility of this complex.

The reaction of **2** with Na⁺[B{3,5-(CF₃)₂C₆H₃}]⁻ (NaBARF₄) at room temperature in MeCN produced the highly electrophilic cationic complex [Mo(NO)(PNP)(NCMe)₃]⁺[BARF₄]⁻ (**3**) with concomitant formation of Na₂[Zn₂Cl₆] in high yield (90%). Complex **3** is quite soluble in THF, toluene, benzene, and chlorobenzene. The ³¹P{¹H} NMR spectra exhibited a single resonance at δ = 52 ppm owing to the equivalence of the phosphorus atoms of the DPEphos ligand. The ³¹P{¹H} NMR signal of **3** did not display a significant shift when compared to **2**. This could presumably be due to a rather loose ion pairing interaction in **2** and **3**. Nevertheless, the exchange of the counterion was confirmed from ¹³C{¹H} NMR spectra and X-ray diffraction studies. Red single crystals suitable for an X-ray diffraction study of **3** were obtained from a toluene/pentane mixture at -30 °C. The X-ray structure analysis of **3** (Figure 1) exhibited pseudo octahedral coordination around the metal center similar to **2**. The phosphorus atoms of the DPEphos ligand and the two MeCN ligands were located in the “equatorial” plane.

The average Mo–N bond length of the acetonitrile ligands was found to be 2.196(2) Å, which is a little longer than the corresponding values of **2**. Similar to **2** the “axially” coordinated MeCN ligand trans to NO was found to be at a slightly longer distance than the “equatorially” coordinated ones.

Catalytic Hydrosilylation Reactions of Aldehydes and Ketones. Various attempts were made to use **3** as a catalyst in olefin hydrogenations, but all of them were unsuccessful. However, **3** was found to catalyze a surprisingly great variety of hydrosilylations. In an optimization series **3** was tested using benzaldehyde and triethylsilane in a 1:1.2 ratio and a loading of 1 mol % of **3**. The reaction was carried out at 120 °C in C₆D₅Cl over 3 h to obtain the corresponding silyl ether, triethyl-(benzyloxy)silane in 100% yield as revealed from the ¹H NMR spectra (Table 1, entry 1). However, the achieved initial turnover frequency (TOF) was quite low (54 h⁻¹). Acetophenone was found to be even less active and required

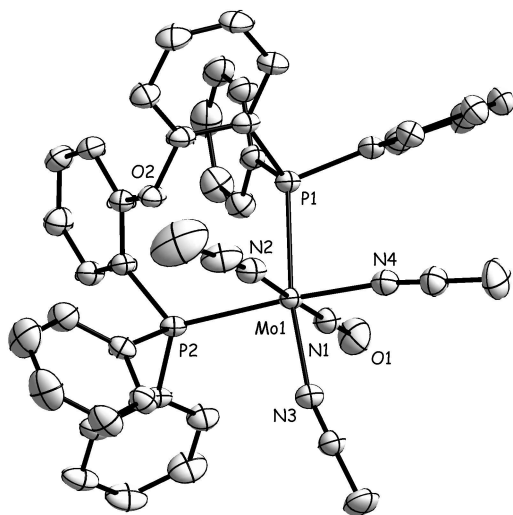
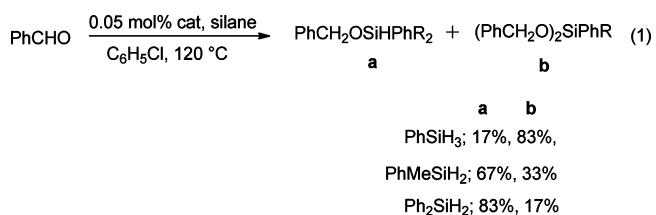


Figure 1. Molecular structure of the cationic part of **3**. Thermal ellipsoids are drawn at the 50% probability level. All hydrogen atoms, solvent molecule, and BARF_4 counteranion are omitted for clarity. Selected bond distances (Å) and bond angles (deg): Mo1–N1 1.7691(19), Mo1–N2 2.236(2), Mo1–N3 2.1839(18), Mo1–N4 2.1675(19), Mo1–P1 2.4794(5), Mo1–P2 2.5156(5), N1–O1 1.221(2), N1–Mo1–N2 177.22(8), N3–Mo1–N4 79.24(7), P1–Mo1–P2 96.857(18), P1–Mo1–N3 170.16(5), P1–Mo1–N2 90.77(5).

a longer reaction time for full conversion (Table 1, entry 2). To improve the activity we screened various solvents. Toluene, THF, and dimethylsulfoxide (DMSO) could not increase the catalytic activity significantly. When MeCN was used as a solvent, conversion of benzaldehyde to the corresponding silyl ether could not be observed as revealed by ^1H NMR (Table 1, entry 5). Temperature was suspected to play a crucial role to

promote the catalytic transformations. Addition of 1 mol % of catalyst **3** to a solution of PhCHO and Et_3SiH (1:1.2) in $\text{C}_6\text{D}_5\text{Cl}$ at room temperature did not furnish any hydrosilylated products after 20 h of reaction time. When eventually the temperature was raised to 80 °C, 16% conversion was observed after 3 h with an initial TOF of 2 h^{-1} (Table 1, entry 7). In addition to these efforts to improve the activity, various silanes were then screened.

The primary aromatic silane PhSiH_3 was found to be highly effective in the hydrosilylation of benzaldehyde. A loading of 0.05 mol % of the catalyst **3** led to 100% conversion of benzaldehyde to the corresponding silyl ether with a maximum TOF of 3520 h^{-1} . However, because of the presence of more than one H_{Si} atoms, formation of $\text{PhCH}_2\text{OSiPhH}_2$ (17%) and $(\text{PhCH}_2\text{O})_2\text{SiPhH}$ (83%) products were observed as revealed by the GC-MS and the ^1H NMR spectra. The secondary silanes, Ph_2SiH_2 and PhMeSiH_2 , were also found to be quite active in the hydrosilylations of benzaldehyde. Nevertheless, in both cases monosilylated products were predominantly formed (eq 1, monosilylated, **a**; disilylated, **b**).



Among the tertiary silanes, trimethoxysilane appeared to be more active compared to other silanes. A loading of 0.2 mol % of catalyst **3** to a mixture of benzaldehyde and $\text{HSi}(\text{OMe})_3$ (1:1.2) in chlorobenzene at 120 °C, revealed full conversion in less than 2 h with an initial TOF of 560 h^{-1} (Table 1, entry 15). The sterically hindered aromatic silanes diphenylmethylsilane

Table 1. Optimization Reactions for the Hydrosilylation of Benzaldehyde Catalyzed by **3**

entry ^a	cat (mol %)	silane	solvent	TOF (h^{-1}) ^b	time (h)	conv (%) ^c	yield (%) ^c
1	1	Et_3SiH	$\text{C}_6\text{D}_5\text{Cl}$	54	3	100	100
2 ^d	1	Et_3SiH	$\text{C}_6\text{D}_5\text{Cl}$	22	11	100	100
3	1	Et_3SiH	THF	46	12	78	78
4	1	Et_3SiH	toluene	38	3	82	82
5	1	Et_3SiH	MeCN		4	0	0
6	1	Et_3SiH	DMSO	10	4	59	59
7 ^e	1	Et_3SiH	$\text{C}_6\text{D}_5\text{Cl}$	2	3	16	16
8	0.05	Ph_2SiH_2	$\text{C}_6\text{D}_5\text{Cl}$	1860	1	100	83/17 ^f
9	0.05	PhSiH_3	$\text{C}_6\text{D}_5\text{Cl}$	3520	1	100	33/67 ^f
10	0.05	PhMeSiH_2	$\text{C}_6\text{D}_5\text{Cl}$	2512	1.5	100	67/33 ^f
11	0.05	PhMeSiH_2	THF	800	0.5	20	20/0 ^f
12 ^g	0.5	PhMeSiH_2	$\text{C}_6\text{D}_5\text{Cl}$	2.5	16	20	20
13	0.2	PhMe_2SiH	$\text{C}_6\text{D}_5\text{Cl}$	290	3	100	100
14	0.2	Ph_2MeSiH	$\text{C}_6\text{D}_5\text{Cl}$	30	17	15	15
15	0.2	$\text{HSi}(\text{OMe})_3$	$\text{C}_6\text{D}_5\text{Cl}$	560	<2	100	100
16	1	$^i\text{Pr}_3\text{SiH}$	$\text{C}_6\text{D}_5\text{Cl}$		0.5	0	0
17	0.2	$\text{HSi}(\text{SiMe}_3)_3$	$\text{C}_6\text{D}_5\text{Cl}$		0.5	0	0
18	0.2	Ph_3SiH	$\text{C}_6\text{D}_5\text{Cl}$	0	3	0	0
19 ^h	0.05	PhMeSiH_2	$\text{C}_6\text{D}_5\text{Cl}$			0	0

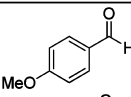
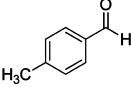
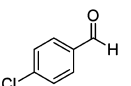
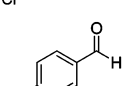
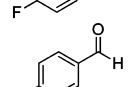
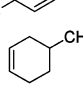
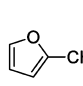
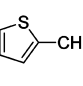
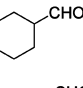
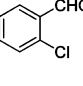
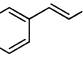
^aUnless otherwise stated 3 mg of the catalyst **3**, benzaldehyde as substrate (given ratio with respect to the catalyst according to Table 1), 1.2 equiv of the silane with respect to substrate, 0.4 mL of solvent, and 120 °C temperature were used as reaction conditions. ^bInitial TOFs were determined from the ^1H NMR spectra after 30 min. ^cConversions and yields were determined from ^1H NMR spectra. ^dAcetophenone was used as substrate. ^e80 °C. ^fRatio of monosilylated and disilylated products (**a/b**) determined by GC/MS. ^gThe reaction was carried out at room temperature, and average TOF was calculated after 16 h. ^hNo catalyst was used.

and phenyldimethylsilane turned out to be less active toward hydrosilylation of benzaldehyde (Table 1, entries 13 and 14).

Catalysis was suppressed with the more sterically encumbered triphenylsilane, triisopropylsilane, and tris(trimethylsilyl)silane (Table 1, entries 16, 17, and 18) even at higher temperatures. A blank experiment using PhMeSiH₂ and benzaldehyde at 120 °C did not show any hydrosilylation product as checked by ¹H NMR and GC/MS. The reaction of benzaldehyde with PhMeSiH₂ using 3 was then carried out in THF at 120 °C, which resulted in a decrease of the TOF value (800 h⁻¹, Table 1, entry 11) in comparison with chlorobenzene as the solvent. However it should be mentioned here that at room temperature a higher catalyst loading (0.5 mol % 3) led to some activity in the hydrosilylation of benzaldehyde using PhMeSiH₂, and after 16 h only 20% conversion was observed with the low TOF value of 2.5 h⁻¹ (Table 1, entry 12).

Nevertheless, at optimized conditions using chlorobenzene as a solvent and phenylmethylsilane at a temperature of 120 °C, the catalytic activities of 3 toward various other aldehydes were tested. Several *para* substituted benzaldehydes were converted to their corresponding silyl ethers with excellent rates and yields (Table 2). One hundred percent conversions could be achieved running the reactions for longer times. But in the case of 4-methoxy and 4-cyanobenzaldehydes, longer reaction times led to as yet unidentified byproducts. The electron donating 4-methoxybenzaldehyde was found to be less active than the electron withdrawing *para* fluoro and *para* chlorobenzaldehydes (Table 2, entries 1, 3 and 4). 2-Chlorobenzaldehyde showed the highest activity among the various substituted benzaldehydes to obtain a maximum TOF of 4864 h⁻¹. 3-Cyclohexenecarboxaldehyde and cinnamaldehyde could be hydrosilylated by 3 without attack on the alkene double bond to obtain a maximum TOF of 960 h⁻¹ and 800 h⁻¹ respectively (Table 2, entries 6 and 11). The catalytic performance of 3 in the hydrosilylation of heterocyclic aromatic aldehydes was also tested. The 2-thiophenecarboxaldehyde and 2-furfural were easily converted to their corresponding hydrosilylated products with high turnover frequencies and yields (Table 2, entries 7 and 8). It should be noted that within an initial period of 30 min of the reactions, disilylated products could not be observed by GC/MS nor by ¹H NMR spectroscopy in most cases of the reactions (For entries 7, 8, and 9 where 15% of disilylation were detected within 30 min). Quite naturally as the reaction progressed the amount of disilylation products increased at a rate slower than the monosilylation products. In some cases monosilylated products were obtained exclusively (Table 1, entries 1, 5, 10, and 11). Thus, the performance of 3 in hydrosilylations of various other substrates were additionally screened. Surprisingly, hydrosilylation of ketones turned out to be much more effective with catalyst 3. For instance acetophenone was hydrosilylated with PhMeSiH₂ with a loading of 0.01 mol % of 3 at 120 °C in 53% conversion within 15 min with an initial TOF of 21232 h⁻¹ (Table 3, entry 1) as revealed by GC/MS. 3 was found to also catalyze the hydrosilylation of acetophenone at room temperature. When 0.025 mol % of 3 was loaded to a mixture of acetophenone and PhMeSiH₂ in chlorobenzene, 38% conversion was observed after 1 h with a TOF of 1520 h⁻¹ and within 5 h full conversion of acetophenone to the corresponding hydrosilylated products (Table 3, entry 1) could be achieved. Thus, we tested various other *para* substituted acetophenones at room temperature and at 120 °C. 4-Methoxyacetophenone turned out to be the most active substrate in hydrosilylations catalyzed by 3. At 120 °C a

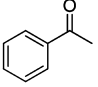
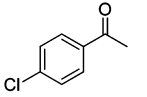
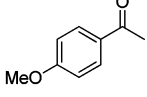
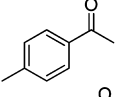
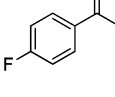
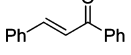
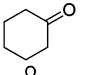
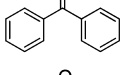
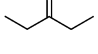
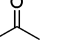
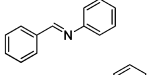
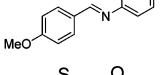
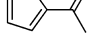
Table 2. Hydrosilylation of Various Aldehydes Catalyzed by 3 Using PhMeSiH₂

$\text{R-CHO} \xrightarrow[\text{PhMeSiH}_2]{0.05 \text{ mol\% cat, } 120^\circ\text{C}} \text{R-OSiHPhMe} + (\text{R-OSiHPhMe})_2$ <div style="text-align: center;"> a b </div>						
Entry ^a	Substrates	Cat (mol%)	TOF (h ⁻¹) ^b	Time (h)	Conv (%) ^c	Yield (%) ^d (a/b)
1		0.05	232	2.5	29	29/0
2		0.05	800	3	89	65/14
3		0.05	1760	2.5	100	82/18
4		0.05	1680	<3	100	57/43
5		0.05	320	2.5	54	54/0
6		0.05	960	7	90	64/26
7		0.05	3600	<2	100	53/47
8		0.05	2720	3	92	67/25
9		0.05	2400	3	88	61/17
10 ^e		0.05	4864	0.25	61	61/0
11		0.05	800	7	100	100/0

^aUnless otherwise stated 3 mg of the catalyst 3, substrate/catalyst ratio according to Table 2, 1.2 equiv of the silane with respect to the substrate, 0.4 mL of C₆H₅Cl and 120 °C temperature. ^bInitial TOFs were calculated by GC/MS after 30 min of reaction time. ^cConversions were determined by GC/MS. ^dYields on the basis of the substrate consumption determined by GC/MS and a/b is the ratio of mono and disilylated products. ^eTOF was determined after initial 15 min.

maximum TOF of 3.2×10^4 h⁻¹ was obtained when 0.01 mol % catalyst 3 was loaded to a mixture of 4-methoxyacetophenone and PhMeSiH₂ (1:1.2) in chlorobenzene. At room temperature, 4-methoxyacetophenone revealed a maximum TOF of 4420 h⁻¹ with a catalyst loading of 0.02 mol % (Table 3, entry 3). Continuing the series of catalyzes with *para* substituted acetophenones as substrates, efficient conversions to the corresponding hydrosilylated products were found to also reach excellent yields within a few hours. Electron withdrawing groups on the *para* position of the acetophenone were slightly less active than *para* electron donating groups on the *para* substituted acetophenones (Table 3, entries 2, 3, 4, and 5). However, unlike the cases of aldehyde hydrosilylation, ketone

Table 3. Hydrosilylation of Various Other Substrates Catalyzed by 3 Using PhMeSiH₂

$ \begin{array}{c} \text{O} \\ \parallel \\ \text{R}_1-\text{C}-\text{R}_2 \xrightarrow[\text{PhMeSiH}_2, \text{ r.t.} - 120^\circ\text{C}]{0.1-0.01 \text{ mol\% cat}} \begin{array}{c} \text{OSiHPhMe} \\ \\ \text{R}_1-\text{C}-\text{R}_2 \\ \\ \text{H} \end{array} \end{array} $						
Entry ^a	Substrate	Cat (mol%)	Temp (°C)	Initial TOF (h ⁻¹) ^b	Time (h)	Yield (%) ^c
1		0.025	r.t.	1520	5	100
		0.01	120	21230	<1	100
		0.01	120	5400 ^d	0.25	13
2		0.025	r.t.	956	1	24
		0.01	120	16320	0.25	40
3		0.02	r.t.	4420	<2	97
		0.01	120	32000	0.5	100
		0.01	120	18400 ^d	0.25	46
4		0.025	r.t.	3200	3	96
		0.01	120	21800	<2	100
5		0.025	r.t.	1480	1	37
		0.01	120	20200	<2	100
6		0.05	120	240	7	77
7		0.1	r.t.	415	5	70
		0.01	120	6800	0.25	17
8		0.025	r.t.	1200	7	100
		0.025	120	8288	<2	100
9		0.1	r.t.	150	24	98
10		0.025	120	12800	<2	92 ^e
		0.1	r.t.	00	14	00
11		0.2	120	110	7	100
12		0.2	120	71	7	100
13		0.1	r.t.	514	5	89
		0.025	120	8000	1.5	96

^aUnless and otherwise stated 0.3 mL of chlorobenzene, 0.5 mg of 3 as catalyst, substrate/catalyst ratio (according to Table 3), 1.2 equiv of PhMeSiH₂ with respect to the substrate, and 120 °C temperature were used as reaction conditions. For room temperature reactions, 1 mg of catalyst 3 was used, and TOFs were calculated from the initial 1st h.

^bTOFs were determined after the initial 15 min of reaction time by GC/MS. ^cYields by GC/MS on the basis of substrate consumption.

^dTHF solvent. ^eIsolated yields.

hydrosilylation brought about exclusively monosilylated products as revealed by GC/MS.

In further studies extension of the scope of the hydrosilylation reactions catalyzed by 3 was explored. Benzophenone, cyclohexanone, 2-acetylthiophene could indeed be converted to their corresponding silyl ether with high activities and yields (Table 3, entries 7, 8, and 13). However, the hydrosilylation of

α,β unsaturated aromatic ketones turned out to be sluggish with a maximum TOF of 240 h⁻¹.

It turned out that imines could be hydrosilylate as well. *N*-benzylideneaniline, and *N*-(4-methoxybenzylidene)aniline were fully converted to their corresponding silylamines within 7 h with a loading of 0.2 mol % of 3 (Table 3, entries 11 and 12). Hydrosilylation could not be observed when styrene and benzonitrile were used as substrates. Applying hydrosilylation reactions with 3 to aliphatic ketones these showed that acetone and 3-pentanone could be converted to the corresponding hydrosilylated products at 120 °C within 7 h in 100% yields as revealed by ¹H NMR and ¹³C NMR spectroscopy (Table 3, entries 9 and 10). With a loading of 0.1 mol % catalyst 3, 3-pentanone was found to be hydrosilylated at room temperature sluggishly showing an initial TOF of 150 h⁻¹, and the reaction went to completion in just 24 h. On the other hand, acetone did not show any activity in hydrosilylation with 3 at room temperature even after 14 h of reaction time and a loading of 0.1 mol % of the catalyst (Table 3, entries 9 and 10).

Kinetic Studies. We carried out three initial kinetic experiments to determine the rate of the hydrosilylation reactions of acetophenone catalyzed by 3 at room temperature varying the concentrations of acetophenone, the silane, and the catalyst. The initial reaction rates were found to be first order with respect to the concentration of the catalyst and the silane. However, the rate was zeroth order with respect to the substrate concentration indicating that catalyst saturation already takes place at low concentration of the substrates. Exemplary kinetic plots are given in Figure 2 (see also Supporting Information).

Based on the kinetic experiments (Table 4) the initial rate equation was established as

$$\text{rate} = 1.131(\text{M}^{-1}\text{min}^{-1})[\text{catalyst}][\text{silane}]$$

Hammett Correlation Study. To understand the influence of various *para* substituted acetophenones, Hammett²³ correlations were established applying catalyst 3 in hydrosilylations of *para*-methoxy, -methyl, -H, -fluoro, and -chloro substituted acetophenones at room temperature and at 120 °C (Figure 3). The initial rates (s⁻¹) were determined from the initial TOF values (s⁻¹). A Hammett plot of ln(rate) vs substituent constant (σ) showed linear correlations with a negative slope (ρ) of -1.14 at 120 °C and -3.18 at room temperature. The Hammett parameters (ρ) indeed reflect the substituent susceptibility of the hydrosilylation processes. A negative ρ value greater than unity indicates a positive charge build up in the transition states and vice versa. The rate limiting step of the hydrosilylation reactions is apparently greatly affected at room temperature by the presence of the electron donating groups in the *para* position of the acetophenone. Naturally, at higher temperature the rate was less sensitive to *para* substitution of the acetophenones (Table 3, entries 1, 2, 3, 4, and 5).

Deuterium Labeling Study. A ²H NMR experiment was performed to confirm that hydride was transferred selectively from the silane moiety. For this purpose, benzaldehyde and Et₃SiD were mixed and heated to 120 °C for 1 h in the presence of catalyst 3 (1 mol %). ²H NMR in chlorobenzene revealed the appearance of a doublet signal at δ 4.8 ppm [²J(¹H, ²H) = 1.8 Hz] corresponding to 27% conversion, which became a singlet in the proton decoupled ²H NMR spectra. This clearly spoke for the transfer of deuterium from the Et₃SiD moiety and formation of PhCHDOSiEt₃.

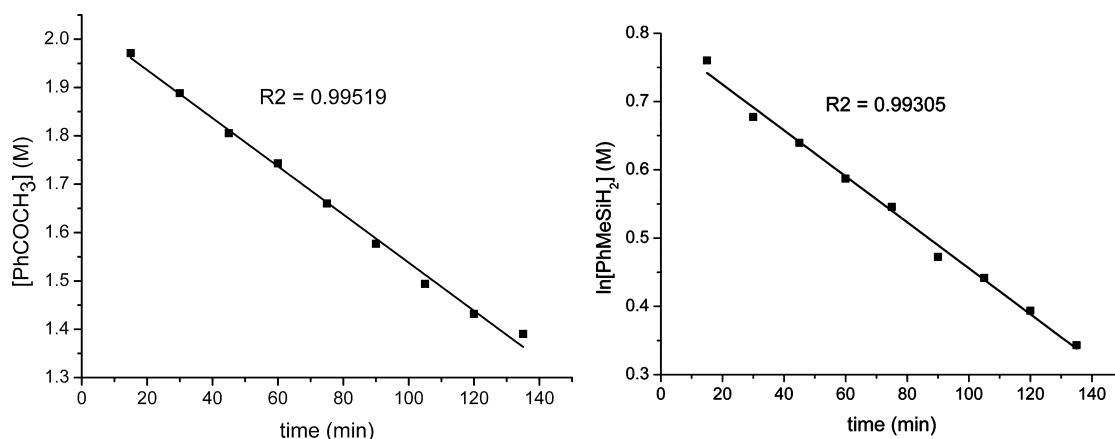


Figure 2. Left: Kinetic plot of $[\text{PhCOCH}_3]$ vs time. Right: Kinetic plot of $\ln[\text{PhMeSiH}_2]$ vs time. $[\text{PhCOCH}_3] = 2.075$ M, $[\text{cat}] = 0.002$ M, $[\text{PhMeSiH}_2] = 2.43$ M. $\text{C}_6\text{D}_5\text{Cl}$ solvent.

Table 4. Dependence of the Initial Rate of Hydrosilylations on the Concentrations of Substrate, Catalyst, and Silane^a

runs	3 (M)	PhMeSiH ₂ (M)	PhC(O)CH ₃ (M)	initial rate (M min ⁻¹)	TOF (h ⁻¹)
1	0.002	2.43	2.075	5.5×10^{-3}	165
2	0.002	4.86	2.075	1.04×10^{-2}	320
3	0.002	2.43	4.14	5.5×10^{-3}	165
4	0.001	2.43	2.075	2.9×10^{-3}	170

^aReactions were carried out at room temperature. Initial rates were determined after 1 h from ^1H NMR integration. Runs 1 and 2, Variation of $[\text{PhMeSiH}_2]$; Runs 1 and 3, Variation of $[\text{PhC(O)CH}_3]$; Runs 1 and 4, Variation of $[\text{Catalyst}]$.

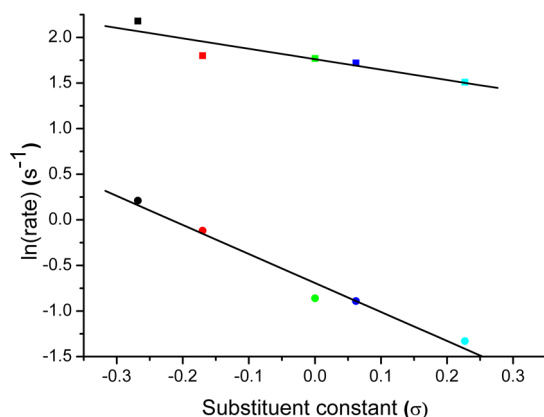


Figure 3. Hammett plot for the hydrosilylation of various *para* substituted acetophenones catalyzed by **3** extracted from initial TOF values. Squares, with $\rho = -1.14$, hydrosilylations at 120 °C. Circles with $\rho = -3.18$, at room temperature. Black: *p*-MeO, red: *p*-CH₃, green: *p*-H, blue: *p*-F, cyan: *p*-Cl groups. PhMeSiH₂ was used as silane.

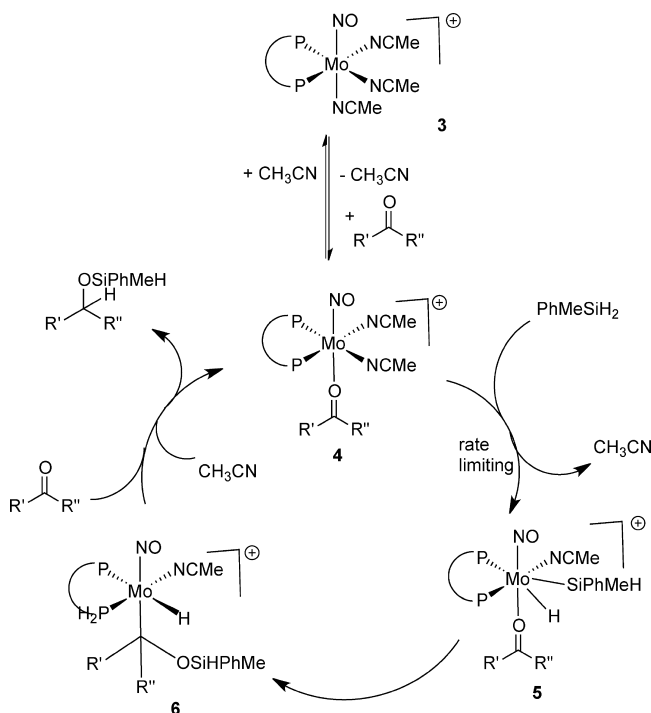
Search for Catalytic Intermediates and Mechanistic Proposal. Additional mechanistic investigations were directed toward detection of catalytic intermediates. When a solution of catalyst **3** (6 mg) in chlorobenzene (or THF), was mixed with 25 equiv of acetophenone at room temperature, the ^{31}P NMR spectra showed appearance of a new singlet signal at δ 52.9 ppm (15%) along with the signal of **3** (δ 50.8 ppm, 85%). This new signal at δ 52.9 ppm could be attributed to the formation of a ketone species of type $[\text{Mo}(\text{NO})(\text{P}(\text{O})\text{Ph})_2(\eta^1\text{-OCPhMe})(\text{NCMe})_2]^+[\text{BAr}^{\text{F}}_4]^-$ (**4**). The ^1H NMR spectra in $\text{C}_6\text{D}_5\text{Cl}$ of the added acetophenone solution revealed the presence of free

acetonitrile which supports the coordination of this ketone to the catalyst **3** via exchange of the labile acetonitrile ligands. When another 80 equiv of acetophenone were added, an additional singlet appeared at δ 52 ppm at the expense of the signal of **3** in the ^{31}P NMR spectra. This could be assigned to a η^2 -acetophenone species $[\text{Mo}(\text{NO})(\text{P}(\text{O})\text{Ph})_2(\eta^2\text{-OCPhMe})(\text{NCMe})_2]^+[\text{BAr}^{\text{F}}_4]^-$. However further addition of acetophenone did not lead to complete disappearance of the complex **3**. This indicated reversible binding of the acetophenone to the molybdenum center. In a similar way, addition of 25 equiv of benzaldehyde to **3** (6 mg) in chlorobenzene (or THF) led to two new doublet signals in the ^{31}P NMR spectra at δ 37 ($J_{\text{PP}} = 98$ Hz) and 30 ppm ($J_{\text{PP}} = 98$ Hz) with complete disappearance of the ^{31}P NMR resonance of **3** indicating stronger coordination of aldehydes to the molybdenum center of **3** liberating acetonitrile as also observed in the ^1H NMR spectra. This stronger binding could be the reason for the lower reactivity of aldehydes in the reported hydrosilylation reactions, although the structure of this new species could not be fully established. Nevertheless we assume that a $[\text{Mo}(\text{NO})(\text{P}(\text{O})\text{Ph})_2(\eta^1\text{-OCHPh})(\text{NCMe})_2]^+[\text{BAr}^{\text{F}}_4]^-$ species had formed where the coordinated aldehyde resides in the equatorial plane trans to one of the phosphorus atoms of DPEphos ligand. However addition of excess of PhMeSiH₂ to a solution of **3** in the absence of the ketone or the aldehyde at room temperature did not reveal changes in the ^{31}P NMR which may exclude initial coordination of the silane to the catalytic center. But when **3** and excess of PhMeSiH₂ were heated at 120 °C, the ^{31}P NMR spectra showed new signals at δ 44 ppm along with signals at δ -9 and δ -17 ppm due to the formation of an as yet unidentified species.

The room temperature hydrosilylation of acetophenone catalyzed by **3** (1 mol %) using PhMeSiH₂ revealed in the ^{31}P NMR spectra the presence of the signals mentioned above (δ 52.9, 52, and 50.8 ppm) throughout the hydrosilylation process and after completion of the hydrosilylation reaction only the signal of **3** (50.8 ppm) was observed. In a similar way when **3**, acetophenone (300 equiv with respect to the catalyst), and PhMeSiH₂ were heated at 120 °C for one minute, the ^{31}P NMR instantly revealed the presence of **3** along with the δ 52.9 and 52 signals before the reaction went to completion. However at the end of the reaction a weak unidentified signal at δ 49 ppm (10%) appears (presumably a product of the reaction of excess silane with **3**), the intensity of which

increases with heating for longer period of times with concomitant decrease of the ^{31}P NMR signal of **3**. Therefore it became obvious that catalyst **3** is the resting state of the catalytic cycle, and **4** (Scheme 2) could be the active species

Scheme 2. Proposed Ojima Type Mechanism for the Hydrosilylation Reactions Catalyzed by 3



before the rate limiting step which may therefore accumulate during the catalysis. To further support this observation another kinetic run was also pursued by ^{31}P NMR using benzophenone as the substrate. Similar to the acetophenone experiment, when 100 equiv of benzophenone was added to a $\text{C}_6\text{D}_5\text{Cl}$ solution of the catalyst **3** (6 mg) the red solution immediately becomes dark green and the ^{31}P NMR spectra of the green solution revealed appearance of two new singlet signals at δ 47.6 and 53.3 ppm (20%) along with a signal for **3**. Further addition of benzophenone does not increase the intensity of these above-mentioned signals as indicated by ^{31}P NMR spectra. Then PhMeSiH_2 was added (1.2 equiv with respect to benzophenone) to this dark green solution and monitored by ^{31}P NMR spectroscopy at room temperature. Similar to the acetophenone case, the above-mentioned two signals at δ 47.6 and 53.3 ppm along with **3** persist throughout the catalysis, and at the end of the reaction only the signal of **3** was observed regenerating the red color of the catalyst.

Furthermore, to get insight into the rate limiting step, a deuterium kinetic isotope effect experiment was also carried out for the hydrosilylation of acetophenone using triethylsilane at 120°C in chlorobenzene. A loading of 1 mol % of the catalyst **3** with acetophenone in presence of Et_3SiH (1.2 equiv) led to formation of a hydrosilylated product corresponding to a conversion of 52% after 3 h. Under similar conditions use of Et_3SiD gave 25% of hydrosilylated product after 3 h as indicated by GC/MS resulting in a DKIE ($k_{\text{H}}/k_{\text{D}}$) value of 2.1. This relatively high DKIE value led us to propose oxidative addition of the silane to **4** type complexes as the rate limiting step. This was in fact also supported by the Hammett

correlation study by the rate enhancement using electron donating *para* substituted acetophenone since the electron donating groups makes the metal center more electron rich facilitating the oxidative addition of the silane to form species **5** (Scheme 2).

On the basis of the Hammett correlation, kinetic study, and our mechanistic observations described just before, an Ojima type^{2,3} mechanism is proposed (Scheme 2) for the hydrosilylation of ketones and aldehydes catalyzed by **3** where oxidative addition of the silane is assumed to be rate limiting. **3** takes the role of a precatalyst and resting state. Then initial exchange of one MeCN ligand by the substrate takes place via a **4** type structure followed by rate limiting oxidative addition of a silane molecule replacing another acetonitrile ligand. A consecutive silyl transfer and H-shift with the subsequent reductive elimination generates the silyl ethers.

CONCLUSION

In conclusion, we have demonstrated that a low-valent cationic molybdenum nitrosyl complex bearing a large bite angle diphosphine and labile MeCN ligands is a highly efficient catalyst in the hydrosilylation of ketones and aldehydes particularly in the presence of the secondary silane PhMeSiH_2 . A great variety of silyl ethers derived from ketones and aryl aldehydes were accessed with good activities and in excellent yields using catalyst **3** at 120°C . Ketones were found to show excellent catalytic performance even at room temperature. Kinetic studies revealed that the rates of the reactions show a first order dependence on the concentration of the catalyst and the silane and are independent of the substrate concentration, which is in agreement with a Ojima type hydrosilylation mechanism.

EXPERIMENTAL SECTION

General Considerations. All manipulations were carried out under an atmosphere of nitrogen using either standard Schlenk techniques or in a glovebox. All reagent grade solvents were dried according to standard laboratory procedure and distilled prior to use under N_2 atmosphere. Deuterated solvents were dried with sodium benzophenone ketyl (THF- d_8 , toluene- d_8 , C_6D_6) and calcium hydride ($\text{C}_6\text{D}_5\text{Cl}$ and CD_2Cl_2) and distilled *via freeze-pump-thaw* cycle prior to use. The DPEphos ligand and $\text{Mo}(\text{NO})\text{Cl}_3(\text{NCMe})_2$ were prepared according to literature procedures.^{22b} All other chemicals were purchased from commercially available sources and used without further purifications. NMR spectra were measured with a Varian Mercury 200 spectrometer (200.1 MHz for ^1H , 81.0 MHz for ^{31}P), with Varian Gemini-300 instrument (^1H at 300.1 MHz, ^{13}C at 75.4 MHz), with a Bruker-DRX 500 spectrometer (500.2 MHz for ^1H , 202.5 MHz for ^{31}P , 125.8 MHz for ^{13}C), and a Bruker-DRX 400 spectrometer (400.1 MHz for ^1H , 162.0 MHz for ^{31}P , 100.6 MHz for ^{13}C). All chemical shifts for ^1H and $^{13}\text{C}\{^1\text{H}\}$ are expressed in ppm relative to tetramethylsilane (TMS) and for $^{31}\text{P}\{^1\text{H}\}$ relative to 85% H_3PO_4 as an external standard reference. Signal patterns are as followed: s, singlet; d, doublet; t, triplet; q, quartet; m, multiplet. IR spectra were obtained either ATR or KBr methods using Biorad FTS-45 instrument. Elemental analyses were carried out at Anorganisch-Chemisches Institut of the University of Zürich. The GC/MS spectra were recorded on a Varian Saturn 2000 spectrometer equipped with Varian 450-GC chromatograph.

[Mo(NO)(P(OP)Cl₂)₂][μCl]₂ (P(OP) = DPEphos) (**1**). Mo(NO)-Cl₃(NCMe)₂ (0.200 g, 0.636 mmol) was dissolved in 10 mL of THF. A solution of DPEphos (0.342 g, 0.635 mmol) in 5 mL of THF was added into that solution. The resulting mixture was kept stirring for 3 h at room temperature. The formed precipitate was filtered off and was washed first with minimum amount of THF and then with pentane. Finally the solid was dried in vacuo to obtain **1** in 86% yield (0.420 g). IR (cm⁻¹, ATR): 1664 (ν_{NO}). Anal. Calcd for [C₃₆H₂₈Cl₃MoNO₂P₂]₂: C, 56.09; H, 3.66; N, 1.82. Found: C, 56.21; H, 3.75; N, 1.68.

[Mo(NO)(P(OP)(NCMe)₃)] [Zn₂Cl₆]_{1/2} (P(OP) = DPEphos) (**2**). To a suspension of **1** (0.20 g, 0.129 mmol) in 10 mL of MeCN, zinc granules (10 equiv) were added. The resulting mixture was kept overnight in acetonitrile with constant stirring at room temperature. After completion of the reaction the solution was filtered off, the solvent was removed in vacuo, and washed with pentane. The solid residue was dissolved in THF and filtered off. The pure product was obtained as an orange powder after removal of the THF in vacuo in 84% yield (0.209 g). IR (cm⁻¹): 1593 (s, ν(NO)). ¹H NMR (500 MHz, THF-*d*₈, 293K): δ 7.52- (broad singlet, Ph), 7.42–7.39 (m, Ph), 7.34–7.30 (m, Ph), 7.26–7.22 (m, Ph), 7.21–7.17 (m, Ph), 7.1 (m, Ph), 7.04–7.02 (m, Ph), 6.95–6.92 (m, DPEphos H), 6.58 (broad singlet, DPEphos H), 2.01 (broad singlet, 9H, CH₃) ppm. ³¹P{¹H} NMR (125 MHz, THF-*d*₈, 20 °C): δ 53.5 (s). ¹³C{¹H} NMR (125.8 MHz, THF-*d*₈, 293K): δ = 159.3 (m, Ph), 135 (m, Ph), 134 (m, Ph), 132 (m, Ph), 130 (m, Ph), 129 (m, Ph), 128.8 (m, Ph), 124 (m, DPEphos), 123 (m, CN), 120 (m, DPEphos), 0.75 (m, CH₃) ppm. Anal. Calcd for C₄₂H₃₇Cl₃MoN₄O₂P₂Zn (959.41): C, 52.58; H, 3.89; N, 5.84. Found: C, 52.53; H, 3.97; N, 5.64.

[Mo(NO)(P(OP)(NCMe)₃)] [BARF₄]₁ (P(OP) = DPEphos) (**3**). Mo-(NO)(DPEphos)(NCMe)₃ [Zn₂Cl₆]_{1/2} (0.070 g, 0.072 mmol) was dissolved in 10 mL of acetonitrile. NaBARF₄ (0.080 g, 0.09 mmol) dissolved in 10 mL of acetonitrile was added to that solution with constant stirring and kept stirring overnight. Then the solution was filtered off, the solvent was removed in vacuo and washed with pentane. The obtained product was extracted with toluene, concentrated, and kept refrigerated (layering with pentane) to reveal pure red colored crystals of **3** in 90% yield. IR (cm⁻¹): 1595 (NO). ¹H NMR (500 MHz, THF-*d*₈, 293K): δ 7.79 (s, BARF₄), 7.58 (s, BARF₄), 7.38 (m, Ph), 7.28 (m, Ph), 7.22 (m, Ph), 7.12 (m, Ph), 7.0 (m, Ph), 6.7 (m, DPEphos H), 2.16 (s, 3H, CH₃), 1.41 (s, 6H, CH₃), ppm. ³¹P{¹H} NMR (162 MHz, THF-*d*₈, 20 °C): δ 52 (s). ¹³C{¹H} NMR (100.8 MHz, THF-*d*₈, 293K): δ = 163 (q, *i*-BARF₄, ¹J_{BC} = 50.0 Hz), Ph 159 (m, Ph), 135 (m, Ph), 133 (m, Ph), 132 (m, Ph), 130 (m, Ph), 129 (m, Ph), 128.8 (m, Ph), 127 (m, BARF₄), 125 (m, DPEphos), 123 (s, CN), 121 (s, BARF₄), 120 (m, CN), 118 (m, DPEphos), 3.06 (s, CH₃), 0.62 (s, CH₃) ppm. Anal. Calcd for C₇₄H₄₉BF₂₄MoN₄O₂P₂ (1650.89): C, 53.84; H, 2.99; N, 3.39. Found: C, 53.75; H, 2.92; N, 3.20.

X-ray Diffraction Analyses. Single-crystal X-ray diffraction data were collected at 183(2) K on an Agilent Technologies Xcalibur Ruby area-detector diffractometer using a single wavelength Enhance X-ray source with MoKα radiation (λ = 0.71073 Å).²⁴ The selected suitable single crystals were mounted using polybutene oil on a flexible loop fixed on a goniometer head and immediately transferred to the diffractometer. Pre-experiment, data collection, data reduction, and analytical absorption correction²⁵ were performed with the program suite CrysAlisPro.²⁶ The structures were solved by

direct methods using SHELXS97.²⁷ The structure refinements were performed by full-matrix least-squares on *F*² with SHELXL97.²⁷ PLATON²⁸ was used to check the result of the X-ray analysis. All programs used during the crystal structure determination process are included in the WINGX software.²⁹ For more details about the data collections and refinements parameters, see the Crystallographic Information files (Supporting Information). Crystallographic data have been deposited with the Cambridge Crystallographic Data Center as CCDC-921393 (for **2**) and CCDC-921394 (for **3**); they contain the supplementary crystallographic data (excluding structure factors) for this paper. These data can be obtained free of charge from The Cambridge Crystallographic Data Center via www.ccdc.cam.ac.uk/data_request/cif

General Procedures for the Catalytic Hydrosilylation Reactions. Table 1: Appropriate amounts of the catalyst **3** (3 mg) and substrate at a given ratio with the catalyst **3**, 1.2 equiv of the silane with respect to the substrate in deuterated solvents (0.4 mL) were placed in a Young tap NMR tube. The reaction mixture was heated to 120 °C. The TOF was determined after initial 30 min of reaction times by ¹H NMR spectroscopy. After the reaction (reaction times according to Table 1), the resulting solution was analyzed by ¹H NMR spectroscopy. The resonances were in accord with those of the literature. The yields were determined by integration of the ¹H NMR spectra on the basis of substrate consumption.

Table 2: The reactions were carried out in C₆H₅Cl in a Young Schlenk tube with stirring. The TOF values (after initial 30 min.) and the final yields were determined by GC/MS on the basis of substrate consumption.

Table 3: A fresh stock solution of catalyst **3** (6.5 mg in 650 μL C₆H₅Cl) was prepared. An aliquot (50 μL) of that stock solution was added to a mixture of the ketone and the silane (amount of ketone with respect to catalyst **3** according to Table 3, ketone: silane = 1:1.2) in 250 μL C₆H₅Cl in a Young tap Schlenk tube. Then the Schlenk tube was kept in a preheated oil bath (120 °C) with stirring. After 15 min of reaction time the Schlenk tube was immediately taken out and cooled to room temperature and taken into the glovebox. Without further purification a GC/MS analysis was carried out to determine the yield of the product (on the basis of the substrate consumption). The same reaction mixture was taken out from the glovebox and heated for longer period of reaction times (Table 3) to achieve complete conversions. For room temperature reactions: A fresh stock solution of catalyst **3** (10 mg in 1 mL of C₆H₅Cl) was prepared. An aliquot (100 μL) of that stock solution was added to a mixture of ketone and silane (amount of ketone with respect to catalyst **3** according to Table 3, ratio of ketone: silane = 1:1.2) in 300 μL of C₆H₅Cl in a Young Schlenk tube and kept stirring. The TOFs were determined after the initial 1 h by GC/MS.

General Procedures for the Kinetic Experiments. For kinetic experiments of Figure 2: In a glovebox, catalyst stock solution was freshly prepared in C₆D₅Cl (5 mg in 1.5 mL of C₆D₅Cl) and an aliquot (0.3 mL) amount was added to a mixture of acetophenone and phenylmethylsilane in a Young NMR tube (see Supporting Information). Then the tube was sealed and left at room temperature. The reaction was monitored by ¹H NMR after each certain time intervals. Yields and product concentrations were determined from the integration of the ¹H NMR spectra.

GC/MS Data for the Hydrosilylated Products of Various Substituted Benzaldehydes and Acetophe-

nones (Other Products See Supporting Information). PhCHO: rt = 3.727 min, m/z = 106; PhCH₂OSiPhH₂: rt = 8.519 min, m/z = 213; (PhCH₂O)₂SiPhH: rt = 13.924 min, m/z = 320; PhCH₂OSiPh₂H: rt = 12.534 min, m/z = 289; (PhCH₂O)₂SiPh₂: rt = 24.231 min, m/z = 395; PhCH₂OSiPhMeH: rt = 8.808 min, m/z = 227; (PhCH₂O)₂SiPhMe: rt = 14.109 min, m/z = 333; *p*-MeOC₆H₄CHO: rt = 6.127 min, m/z = 135; *p*-MeOPh-CH₂OSiPhMeH: rt = 10.346 min, m/z = 257; *p*-MeC₆H₄CHO: rt = 4.718 min, m/z = 119; *p*-MePhCH₂OSiPhMeH: rt = 9.420 min, m/z = 241; (*p*-MePhCH₂O)₂SiPhMe: rt = 16.757 min, m/z = 361; *p*-ClC₆H₄CHO: rt = 5.128 min, m/z = 139; *p*-ClPhCH₂OSiPhMeH: rt = 10.039 min, m/z = 261; (*p*-ClPhCH₂O)₂SiPhMe: rt = 22.023 min, m/z = 402; *p*-FC₆H₄CHO: rt = 3.652 min, m/z = 124; *p*-FPhCH₂OSiPhMeH: rt = 8.746 min, m/z = 245; (*p*-FPhCH₂O)₂SiPhMe: rt = 13.741 min, m/z = 369; *p*-CNC₆H₄CHO: rt = 6.019 min, m/z = 131; *p*-CNPhCH₂OSiPhMeH: rt = 10.933 min, m/z = 252; *o*-ClC₆H₄CHO: rt = 5.033 min, m/z = 139; *o*-ClPhCH₂OSiPhMeH: rt = 9.863 min, m/z = 261; PhC(O)-CH₃: rt = 4.560 min, m/z = 120; PhCH(CH₃)OSiPhMeH: rt = 8.634 min, 8.725 min, m/z = 241; *p*-MeOC₆H₄C(O)CH₃: rt = 6.863 min, m/z = 150; *p*-MeOC₆H₄CH(CH₃)OSiPhMeH: rt = 10.115 min, 10.233 min, m/z = 272; *p*-CH₃C₆H₄C(O)CH₃: rt = 5.556 min, m/z = 134; *p*-CH₃C₆H₄CH(CH₃)OSiPhMeH: rt = 9.209 min, 9.320 min, m/z = 255; *p*-FC₆H₄C(O)CH₃: rt = 4.461 min, m/z = 138; *p*-FC₆H₄CH(CH₃)OSiPhMeH: rt = 8.581 min, 8.864 min, m/z = 259; *p*-ClC₆H₄C(O)CH₃: rt = 5.967 min, m/z = 154; *p*-ClC₆H₄CH(CH₃)OSiPhMeH: rt = 9.808 min, 9.930 min, m/z = 275; *p*-CNC₆H₄C(O)CH₃: rt = 6.830 min, m/z = 145; *p*-CNC₆H₄CH(CH₃)OSiPhMeH: rt = 10.696 min, 10.836 min, m/z = 266.

■ ASSOCIATED CONTENT

● Supporting Information

Molecular structure of **2**, the GC/MS data of various other substrates and products, and crystallographic information files of **2** and **3**. This material is available free of charge via the Internet at <http://pubs.acs.org>.

■ AUTHOR INFORMATION

Corresponding Author

*E-mail: hberke@aci.uzh.ch.

Notes

The authors declare no competing financial interest.

■ ACKNOWLEDGMENTS

Financial support from the Swiss National Science Foundation and the funds of the University of Zürich are gratefully acknowledged.

■ REFERENCES

- (1) (a) Chalk, A. J.; Harrod, J. F. *J. Am. Chem. Soc.* **1965**, *87*, 16. (b) Ojima, I.; Nihonyanagi, M.; Nagai, Y. *J. Chem. Soc., Chem. Commun.* **1972**, 938. (c) Ojima, I.; Nihonyanagi, M.; Kogure, T.; Kumagai, M.; Horiuchi, S.; Nakatsugawa, K. *J. Organomet. Chem.* **1975**, *94*, 449. (d) Ojima, I.; Kogure, T. *Organometallics* **1982**, *1*, 1390. (e) Ojima, I.; Kogure, T.; Kumagai, M.; Horiuchi, S.; Sato, Y. *J. Organomet. Chem.* **1976**, *122*, 83.
- (2) Schneider, N.; Finger, M.; Haferkemper, C.; Bellemin-Laponnaz, S.; Hofmann, P.; Gade, L. H. *Chem.—Eur. J.* **2009**, *15*, 11515–11529.
- (3) Berc, S. C.; Kreutzer, K. A.; Buchwald, S. L. *J. Am. Chem. Soc.* **1991**, *113*, 5093.
- (4) (a) Nolin, K. A.; Krumper, J. R.; Pluth, M. D.; Bergman, R. G.; Toste, F. D. *J. Am. Chem. Soc.* **2007**, *129*, 14684. (b) Kennedy-Smith, J. J.; Nolin, K. A.; Gunterman, H. P.; Toste, F. D. *J. Am. Chem. Soc.* **2003**, *125*, 4056. (c) Nolin, K. A.; Ahn, R. W.; Kobayashi, Y.; Kennedy-Smith, J. J.; Toste, F. D. *Chem.—Eur. J.* **2010**, *16*, 9555. (d) Shirobokov, O. G.; Kuzmina, L. G.; Nikonov, G. I. *J. Am. Chem. Soc.* **2011**, *133*, 6487.
- (5) (a) Glaser, P. B.; Tilley, T. D. *J. Am. Chem. Soc.* **2003**, *125*, 13640–13641. (b) Calimano, E.; Tilley, T. D. *Organometallics* **2010**, *29*, 1680–1692.
- (6) (a) Corma, A.; Gonzalez-Arellano, C.; Iglesias, M.; Sanchez, F. *Angew. Chem., Int. Ed.* **2007**, *46*, 7820–7822. (b) Shaikh, N. S.; Enthaler, S.; Junge, K.; Beller, M. *Angew. Chem., Int. Ed.* **2008**, *47*, 2497–2501. (c) Han, J. W.; Tokunaga, N.; Hayashi, T. *J. Am. Chem. Soc.* **2001**, *123*, 12915–12916. (d) Jensen, J. F.; Svendsen, B. Y.; Cour, T. V.; Pedersen, H. L.; Johannsen, M. *J. Am. Chem. Soc.* **2002**, *124*, 4558–4559. (e) Flückiger, M.; Togni, A. *Eur. J. Org. Chem.* **2011**, 4353–4360. (f) Junge, K.; Wendt, B.; Addis, D.; Zhou, S.; Das, S.; Beller, M. *Chem.—Eur. J.* **2010**, *16*, 68–73.
- (7) (a) Ison, E. A.; Trivedi, E. R.; Corbin, R. A.; Abu-Omar, M. M. *J. Am. Chem. Soc.* **2005**, *127*, 15374. (b) Du, G.; Fanwick, P. E.; Abu-Omar, M. M. *J. Am. Chem. Soc.* **2007**, *129*, 5180.
- (8) (a) Roesler, R.; Har, B. J. N.; Piers, W. E. *Organometallics* **2002**, *21*, 4300. (b) Song, Y. -S.; Yoo, B. R.; Lee, G. -H.; Jung, N. *Organometallics* **1999**, *18*, 3109–3115. (c) Parks, D. J.; Blackwell, J. M.; Piers, W. E. *J. Org. Chem.* **2000**, *65*, 3090–3098. (d) Rubin, M.; Schwier, T.; Gevorgyan, V. *J. Org. Chem.* **2002**, *67*, 1936–1940. (e) Asao, N.; Sudo, T.; Yamamoto, Y. *J. Org. Chem.* **1996**, *61*, 7654–7655.
- (9) (a) Gligler, P.; Bechlars, B.; Herrmann, W. A.; Kühn, F. E. *J. Am. Chem. Soc.* **2011**, *133*, 1589–1596. (b) Do, Y.; Han, J.; Rhee, Y. H.; Park, J. *Adv. Synth. Catal.* **2011**, *353*, 3363–3366. (c) Hashimoto, H.; Atani, I.; Kabuto, C.; Kira, M. *Organometallics* **2003**, *22*, 2199–2201. (d) Park, S.; Brookhart, M. *Organometallics* **2010**, *29*, 6057–6064. (e) Gutsulyak, D. V.; Vyboishchikov, S. F.; Nikonov, G. I. *J. Am. Chem. Soc.* **2010**, *132*, 5950–5951. (f) Nishibayashi, Y.; Takei, I.; Uemura, A.; Hidai, M. *Organometallics* **1998**, *17*, 3420–3422. (g) Rieger, K.; Högerl, M. P.; Gligler, P.; Kühn, F. E. *ACS Catal.* **2012**, *2*, 613–621. (h) Gibson, S. E.; Rudd, M. *Adv. Synth. Catal.* **2007**, *349*, 781. (i) Marciniak, B. *Comprehensive Handbook on Hydrosilylation*; Pergamon: Oxford, U.K., 1992.
- (10) (a) Yang, J.; Tilley, T. D. *Angew. Chem., Int. Ed.* **2010**, *49*, 10186. (b) Shaikh, N. S.; Enthaler, S.; Junge, K.; Beller, M. *Angew. Chem., Int. Ed.* **2008**, *47*, 5429. (c) Bhattacharya, P.; Krause, J. A.; Guan, H. *Organometallics* **2011**, *30*, 4720–4729. (d) Buitrago, E.; Tinnis, F.; Adolfsson, H. *Adv. Synth. Catal.* **2012**, *354*, 217–222. (e) Wu, J. Y.; Stanzl, B. N.; Ritter, T. *J. Am. Chem. Soc.* **2010**, *132*, 13214–13216. (f) Dieskau, A. P.; Begouin, J. M.; Plietker, B. *Eur. J. Org. Chem.* **2011**, 5291–5296. (g) Kamata, K.; Suzuki, A.; Nakai, Y.; Nakazawa, H. *Organometallics* **2012**, *31*, 3825–3828. (h) Hashimoto, T.; Urban, S.; Hoshino, R.; Ohki, Y.; Tatsumi, K.; Glorius, F. *Organometallics* **2012**, *31*, 4474–4479. (i) Tondreau, A. M.; Lobkovsky, E.; Chirik, P. J. *Org. Lett.* **2008**, *19*, 2789–2792.
- (11) (a) Carter, M. B.; Schiott, B.; Gutiérrez, A.; Buchwald, S. L. *J. Am. Chem. Soc.* **1994**, *116*, 11667. (b) Yun, J.; Buchwald, S. L. *J. Am. Chem. Soc.* **1999**, *121*, 5640. (c) Halterman, R. L.; Ramsey, T. M.; Chen, Z. *J. Org. Chem.* **1994**, *59*, 2642–2644. (d) Kesti, M. R.; Waymouth, R. H. *Organometallics* **1992**, *11*, 1095–1103.
- (12) (a) Bullock, R. M. *Chem.—Eur. J.* **2004**, *10*, 2366–2374. (b) Bullock, R. M. In *Handbook of Homogeneous Hydrogenation*; de Vries, J. G., Elsevier, C. J., Eds.; Wiley-VCH: Weinheim, Germany, 2007; Chapter 7. (c) Bullock, R. M. *Catalysis without precious metals*; Wiley-VCH: Weinheim, Germany, 2010.
- (13) (a) Dioumaev, V. K.; Bullock, R. M. *Nature* **2000**, *424*, 530–532. (b) Fernandes, A. C.; Fernandes, R.; Romão, C. C.; Royo, B. *Chem. Commun.* **2005**, 213–214. (c) Reis, P. M.; Romão, C. C.; Royo, B. *Dalton Trans.* **2006**, 1842–1846. (d) Ziegler, J. E.; Du, G.; Fanwick,

- P. E.; Abu-Omar, M. M. *Inorg. Chem.* **2009**, *48*, 11290. (e) Costa, P. J.; Romão, C. C.; Fernandens, A. C.; Royo, B.; Reis, P.; Calhorda, M. J. *Chem.—Eur. J.* **2007**, *13*, 3934. (f) Khalimon, A. Y.; Ignatov, S. K.; Simionescu, R.; Kuzmina, L. G.; Howard, J. A. K.; Nikonov, G. I. *Inorg. Chem.* **2012**, *51*, 754–756. (g) Khalimon, A. Y.; Shirobokov, O. G.; Peterson, E.; Simionescu, R.; Kuzmina, L. G.; Howard, J. A. K.; Nikonov, G. I. *Inorg. Chem.* **2012**, *51*, 4300–4313.
- (15) (a) Peterson, E.; Khalimon, A. Y.; Simionescu, R.; Kuzmina, L. G.; Howard, J. A. K.; Nikonov, G. I. *J. Am. Chem. Soc.* **2009**, *131*, 908. (b) Shirobokov, O. G.; Simionescu, R.; Kuzmina, L. G.; Nikonov, G. I. *Chem. Commun.* **2010**, *6*, 7831.
- (16) (a) Jiang, Y.; Hess, J.; Fox, T.; Berke, H. *J. Am. Chem. Soc.* **2010**, *132*, 18233–18247. (b) Choualeb, A.; Maccaroni, E.; Blacque, O.; Schmalke, H. W.; Berke, H. *Organometallics* **2008**, *27*, 3474–3481.
- (17) (a) Dong, H.; Berke, H. *Adv. Synth. Catal.* **2009**, *351*, 1783–1788. (b) Jiang, Y.; Berke, H. *Chem. Commun.* **2007**, 3571–3573.
- (c) Huang, W. J.; Berke, H. *Chimia* **2005**, *59*, 113–115.
- (18) Jiang, Y.; Blacque, O.; Fox, T.; Frech, C. M.; Berke, H. *Chem.—Eur. J.* **2009**, *15*, 2121–2128.
- (19) Jiang, Y.; Blacque, O.; Fox, T.; Frech, C. M.; Berke, H. *Organometallics* **2009**, *28*, 5493–5504.
- (20) Dybov, A.; Blacque, O.; Berke, H. *Eur. J. Inorg. Chem.* **2011**, 652–659.
- (21) Duddle, B.; Rajesh, K.; Blacque, O.; Berke, H. *J. Am. Chem. Soc.* **2011**, *133*, 8168–8178.
- (22) (a) Kranenburg, M.; Burgt, Y. E. M.; van der Kamer, P. C. J.; van Leeuwen, P. W. N. M. *Organometallics* **1995**, *14*, 3081–3089. (b) Bencze, L.; Kohan, J. *Inorg. Chim. Acta* **1982**, *65*, L17–L19.
- (23) (a) Hammett, L. P. *J. Am. Chem. Soc.* **1937**, *59*, 96–103. (b) Hammett, L. P. *Chem. Rev.* **1935**, *17*, 125–136. (c) Hansch, C.; Leo, A.; Taft, R. W. *Chem. Rev.* **1991**, *91*, 165–195. (d) Yang, X.; Zhao, L.; Fox, T.; Wang, Z.-X.; Berke, H. *Angew. Chem., Int. Ed.* **2010**, *49*, 2058.
- (24) *Xcalibur Ruby*; Agilent Technologies (formerly Oxford Diffraction): Yarnton, Oxfordshire, England, 2012.
- (25) Clark, R. C.; Reid, J. S. *Acta Crystallogr., Sect. A* **1995**, *51*, 887.
- (26) *CrysAlisPro*, Version 1.171.36.20; Agilent Technologies: Yarnton, Oxfordshire, England, 2012.
- (27) Sheldrick, G. *Acta Crystallogr., Sect. A* **2008**, *64*, 112.
- (28) Spek, A. L. *J. Appl. Crystallogr.* **2003**, *36*, 7.
- (29) Farrugia, L. *J. Appl. Crystallogr.* **1999**, *32*, 837.